Chapter 5

Cluster emission

In nuclear structure studies the evaporation of α-particles is a decay process which is commonly used to produce residual nuclei, which can be subsequently studied via γ-ray spectroscopy. Less frequently used is the emission of heavier charged clusters, a mechanism which is particularly interesting since it may be able to produce nuclei in states of angular momentum and excitation energy that are not normally populated via light-particle emission. Large γ-ray detector arrays like EUROBALL and GASP often make use of light charged-particle triggers to select a particular γ-decaying nucleus. The detection of γ-rays in coincidence with heavier clusters is generally more difficult requiring the integration of large gas counters with close-packed germanium-detector arrays. To overcome this difficulty we have studied the γ-ray decay of compound nuclei in coincidence with clusters, excited to states just above the particle threshold. As a trigger we have used the cluster decay into 2 or more α-particles. The experiments have been performed at the Laboratori Nazionali di Legnaro, Italy, using the γ-detector array GASP, consisting of 40 high purity Ge detectors and a multiplicity filter of 80 BGO scintillators. Light charged particles have been detected by the ISIS silicon-ball consisting of 40 ΔE-E telescopes each covering a solid angle of about 0.20 sr (29° in the reaction plane). For more information see Chapter 2. Strongly correlated α-particles emitted in the decay of such weakly bound cluster states

will be detected in the same Si telescopes and observed through the pile-up of signals.

Here, results from two different reactions will be presented with the aim of observing ^{8}Be and $^{12}C^{*}_{0_2^+}$ cluster emission.

1) ^{18}O+^{13}C$\rightarrow^{23}$Ne + (^{8}Be or 2α), at an energy of $E_{LAB}(^{18}O)$ = 100 MeV, aimed for the study of Ne isotopes. In the case of ^{8}Be emission one should take into account that we can not distinguish between the ground state, which is unbound by 91.9 keV and the first excited 2^+ state. An estimation of the decay cone for the ^{8}Be (ground state) emission gives approximately 4°. Having a width of 1.5 MeV at an excitation energy of 3.04 MeV the excited 2^+ level will produce an opening cone on average of 24°, this means that just a part of the 2α pairs coming from the decay of such an excited state could be registered in one ISIS-telescope (29°). Furthermore, the emission of ^{6}Li and ^{7}Li has been observed in this reaction.

2) ^{28}Si+^{24}Mg$\rightarrow^{40}$Ca + (^{12}C or 3α) at an incident energy of 130 MeV. Due to the high incident energy the compound nuclear decay favours the emission of several α-particles (up to 3 or 4 α-particles) and the emission of ^{8}Be and ^{12}C fragments, as can be seen from the data shown in Fig. 5.1. This allows the observation of the reaction channel corresponding to the emission of ^{8}Be plus one α-particle, as well as of the $^{12}C^{*}_{0_2^+}$ -state which is localised at an excitation energy of 7.6542 MeV, 288 keV above the 3α threshold. With the instantaneous break-up of this excited 0_2^+-state, 3α particles are emitted in a very narrow cone of only ≈10°, which fits well into the opening angle (29°) of the ISIS-telescopes.

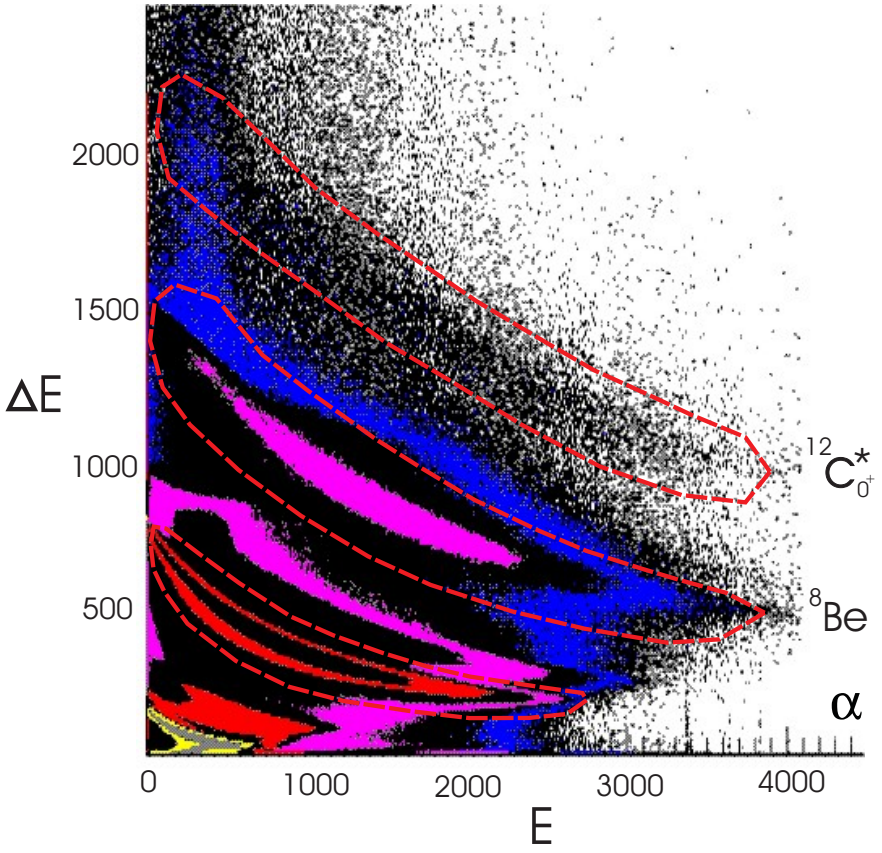

Figure 5.1: A plot of ΔE-E signals from the ISIS telescopes obtained in the ^{28}Si+^{24}Mg experiment.

5.1 Experimental conditions

5.1.1 The ISIS detector and multiple hit events

Absorber foils of 12μm thick aluminium were mounted facing the target to prevent scattered beam particles from penetrating the silicon detectors. The observation of unbound clusters populated close to the decay threshold, such as in beryllium and carbon, becomes possible by the detection of their light decay products. The identification of the decay products, produced by the cluster decay, from the background of evaporated charged particles relies on the former being emitted in a narrow angular cone.

The total solid angle covered by the ISIS detectors is 64% of 4π. Due to the width of the detector frames there is a gap of approximately 6-7° between adjacent detectors. The kinematic conditions (the narrow emission cone) allow us to neglect the contribution from the α-particle events arising from cluster decay products entering 2 neighbouring detectors.

Plotting the energy signal of the first (thin-ΔE) detector versus the signal of the second (thick-E) detector, the events, for each different mZ^2 value, following the Bethe-Bloch formula (see Eq. 2.2), will be separated into a distinct 'banana' shaped distribution (see Figs. 5.1 and 5.2).

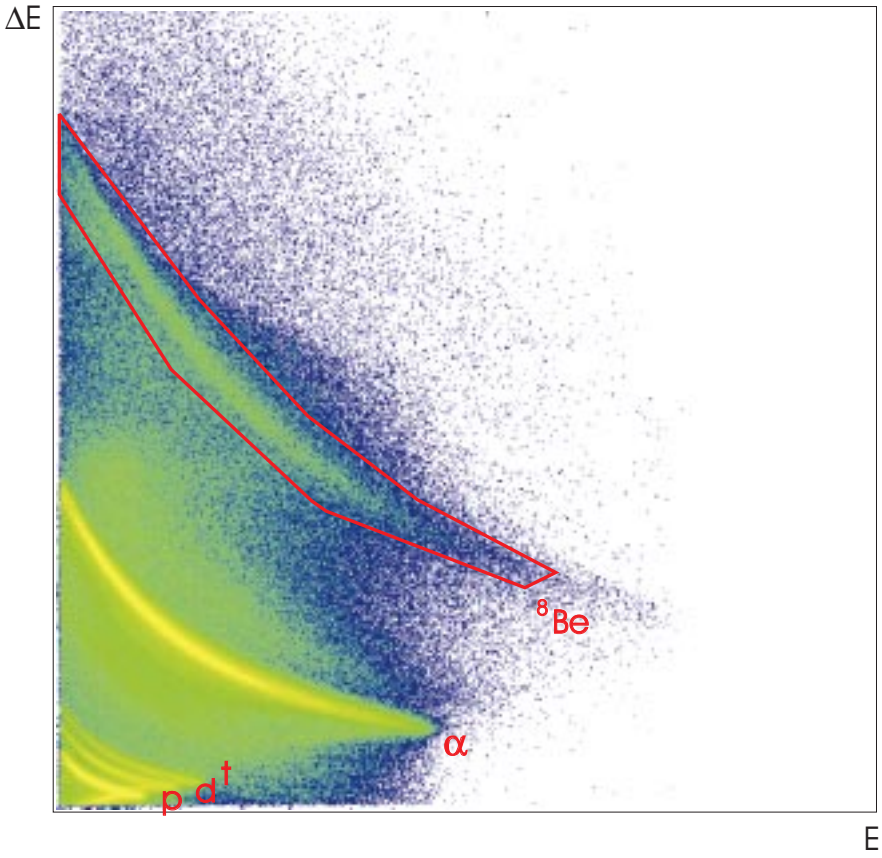

Figure 5.2: A plot of ΔE-E signals from the ISIS telescopes obtained in the ^{18}O+^{13}C experiment.

The majority of the 2α-events (97%) due to cluster decay are observed in

the first 3 rings of the ISIS detectors. Those events are registered as multiple hit-signals in the identification plots, with 2- or 3-times higher values than the original Bethe-Bloch-curves for the single α-particles. In the emission of 2 or 3 α-particles from an unbound state, each α-particle obtains, in their centre of mass frame, an energy of less than 100 keV, the original binary fragment being emitted with an energy of typically 30-50 MeV. The momentum vectors of such α-particles are thus almost the same. As a consequence the multiple hit signals corresponding to the detection of such strongly correlated decay products into the same telescope lie on an event line which corresponds to a rescaling of the ΔE- and E-signals, *i.e.* having a functional dependence described by the Bethe-Bloch formula.

For a quantitative evaluation the probability of having the so called 'multiple hit' events must be discussed. The ISIS spectrometer was built to have a small multiple hit event-rate of less than 2% even for high multiplicities Ref. [Far01]. In Fig. 5.3 the dependence of the probability for multiple hits on the efficiency for different particle-multiplicities is shown. According to the data obtained in the ^{18}O+^{13}C and ^{28}Si+^{24}Mg experiments the event-rate for 2 or 3α-particles registered in the same detector compared to 2 or 3 α-particles observed in different detectors is around 30%.

For N_D number of detectors, each covering a fraction ε of the solid angle, the probability of detecting F (Fold) α-particles of M (Multiplicity) emitted will be:

$$P(F,M) = \binom{M}{F} (N_D\varepsilon)^F (1 - N_D\varepsilon)^{M-F} \tag{5.1}$$

In the case $M = F = 2$ this reduces to the total probability of detecting 2 out of 2 particles in all detectors:

$$P(2,2) = (N_D\varepsilon)^2 \tag{5.2}$$

The probability of detecting 2 out of 2 particles in separate detectors is:

$$P_{sh}(2,2) = N_D(N_D - 1)\varepsilon^2 \tag{5.3}$$

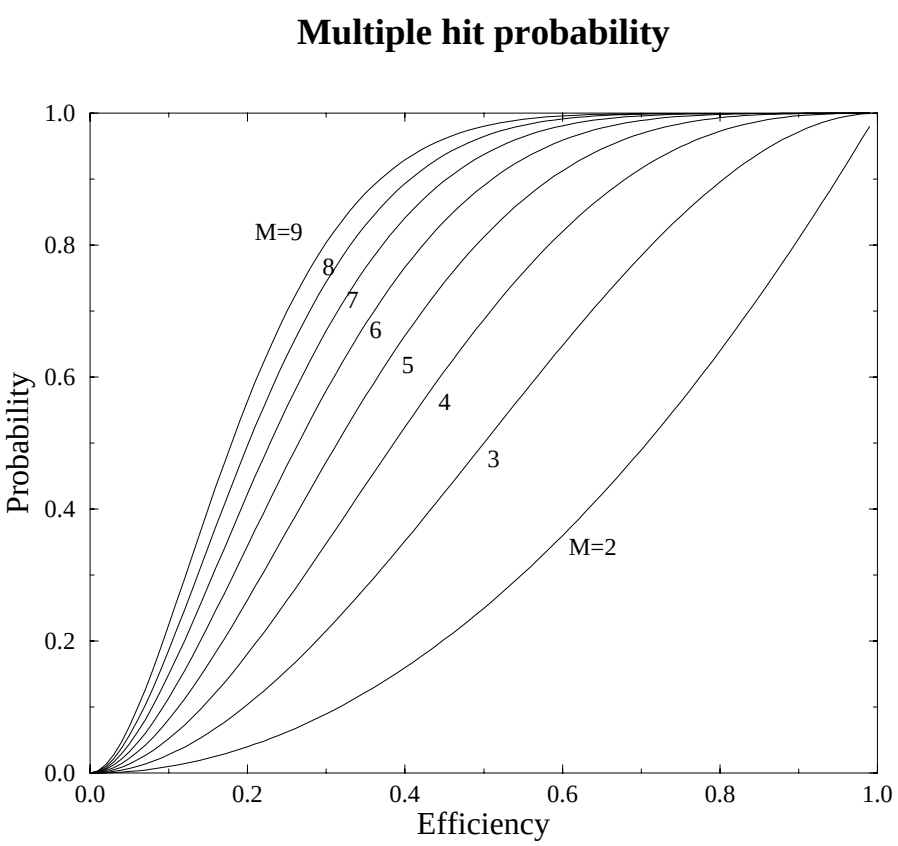

Figure 5.3: The probability of a multiple hit for a single segment covering a solid angle of $\Omega = 4\pi$ as a function of the efficiency of the segment, for various values of the emitted particle multiplicity (M) [Far01].

According to this the probability of double hits in single detectors will be:

$$P_{dh}(2,2) = P(2,2) - P_{sh}(2,2) = N_D\varepsilon^2 \tag{5.4}$$

Thus, the ratio of chance double hits compared to registering the two particles in separate detectors (for equal and isotropic probability for emitting a single particle) is:

$$\frac{P_{dh}(2,2)}{P_{sh}(2,2)} = \frac{1}{N_D - 1} \tag{5.5}$$

which is independent of ε.

One can assume that the probability of detecting 2α-particles coming from

^{8}Be is

$$P(^{8}Be) = N_D\varepsilon \tag{5.6}$$

Thus one can build the ratio of the probability of detecting 2 out of 2 particles in different detectors to the probability of detecting ^{8}Be:

$$\frac{P_{sh}(2,2)}{P(^{8}Be)} = (N_D - 1)\varepsilon \tag{5.7}$$

The same considerations can be made for the emission of 3α particles and ^{12}C*. In this case for F=M=3 the total probability is:

$$P(3,3) = (N_D\varepsilon)^3 \tag{5.8}$$

For detecting three particles in different detectors in this case the probability is given by:

$$P_{sh}(3,3) = N_D(N_D - 1)(N_D - 2)\varepsilon^3 \tag{5.9}$$

Thus, building the difference from these two equations (5.8 and 5.9) one can obtain the probability of triple hits:

$$P_{trh}(3,3) = P(3,3) - P_{sh}(3,3) = N_D(3N_D - 2)\varepsilon^3 \tag{5.10}$$

For the detection of ^{12}C*, since the particles are emitted together the probability is, as in the case of ^{8}Be,

$$P(^{12}C) = N_D\varepsilon \tag{5.11}$$

The contribution of random coincidences in the same telescope coming from uncorrelated evaporated α-particles with different energies will be distributed over a wider region in the ΔE-E plots. Here one observes a deviation from the Bethe-Bloch function as shown schematically in Fig. 5.4. The energy spectrum of the multiple hit events in this case is given by:

$$N(E) = N_1(E_i)E_i + N_2(E_j)E_j \tag{5.12}$$

For the same total energy, $E = (E_i + E_j)$, the final distribution will not follow the Bethe-Bloch dependence of $\Delta E \sim mZ^2/E$ because of the non linear dependence $(1/E)$ of the ΔE-signal.

This deviation can be clearly seen by constructing the multiple hit events using 2 very different values of the energies for the 2 detected α-particles: in the case of an uncorrelated emission the energies of the two α-particles may be very different (B1 and B2 in Fig 5.4). Here, E(multiple hit)=B1+B2 (see Fig. 5.4). This implies that chance coincidences start to deviate towards higher ΔE values with respect to the rescaled Bethe-Bloch line of the ^{8}Be. A similar effect is expected for the ^{12}C-line, although here the probability of chance coincidences for 3 α-particles contributing to the cluster decay event line must be very small (see Fig. 5.1). In Figs. 5.1 and 5.2 the plots of the charged particle identification events are shown for the two reactions as was observed with the ISIS silicon-telescopes, which illustrate these considerations.

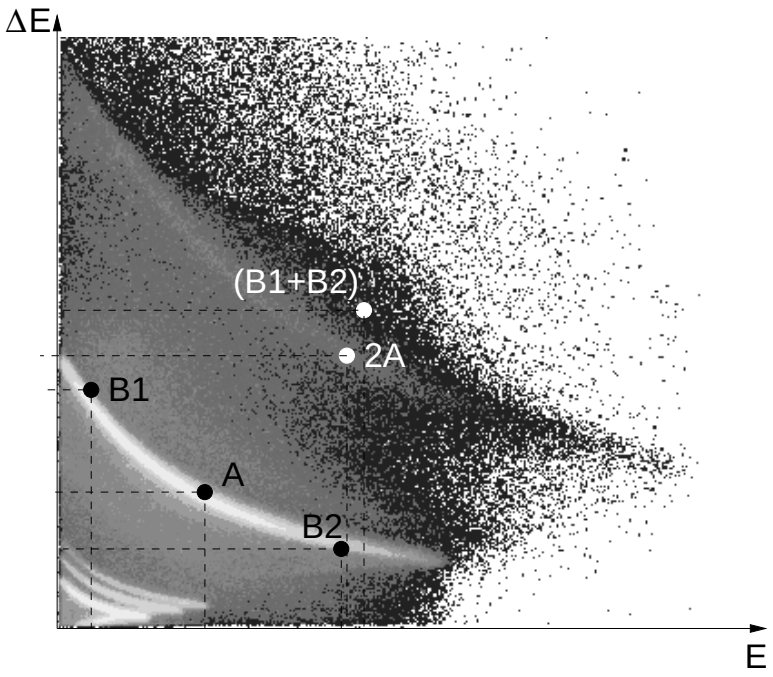

Figure 5.4: Schematic illustration of the deviation of the random multiple hit events from the event line of the coincident α-particles from the ^{8}Be-emission. Two ΔE-E-signals for different energies (cases B1 and B2) and for equal energies (case A), are chosen, as indicated.

In the case of ^{8}Be and ^{12}C emission the energies of the emitted α-particles and the corresponding energy spectra are:

$$E_i = E_j = E_k$$
$$N_1(E_i) = N_2(E_j) = N_3(E_k) \tag{5.13}$$

For uncorrelated α-particles evaporated with almost the same energies no deviation from the Bethe-Bloch formula will be observed. These events will lie in the '^{8}Be' banana. According to Eq. 5.13, for the comparison between these multiple hit events and ^{8}Be or ^{12}C one can take the rescaled (by factor of 2 or 3 times respectively) energy spectrum for 1 α-particle.

In addition to the true ^{8}Be and ^{12}C lines, there will still be events from sequential compound nucleus emissions which can produce chance coincidences, with events of 2 and 3 α-particles with the same energies, which will not deviate from the rescaled Bethe-Bloch line to larger ΔE-values. In order to assess these contributions a simple formula for chance coincidences, N^{random}, can be used.

$$N_{2\alpha}^{random}(E) = N_{\alpha}^{2}(E)\Delta\tau \tag{5.14}$$

The counting rates N_α can be taken from the running time and the total events in the α-particle line. The integration time, $\Delta\tau$, in the electronic amplifier creating the signals is $\sim$90 ns. Thus the calculated value for $N_{2\alpha}^{random}$ is less than 0.03% and can be neglected. This means that each event contains coincidences from just one reaction.

5.2 Results and discussion of cluster emission as a statistical process

5.2.1 Discussion of the charged particle spectra

Using the calibrated ΔE-E -signals we have compared the total energy spectra of the reconstructed fragment emissions with the expected multiple random events due to the detection of 2 or more evaporated α-particles. For the latter it is assumed that double or triple events are obtained by rescaling the energy of a single α-particle by a factor of 2 or 3 respectively see Eq. 5.13. As shown in Figs. 5.5 and 5.6 the two curves have different shapes and maxima.

Thus, from Equation 5.5, looking at a channel with true multiplicity 2 it is not possible to extract the efficiency from the ratio, because this actually depends only on the number of detectors. Using only the 6 forward detectors (ring 1 in ISIS) the energy dependence of this ratio in the upper part of the spectrum for the emission of 2 α-particles should tend towards 0.2 (=1/(6−1)). A deviation from this value will indicate that more processes contribute to the double hit, namely cluster emission.

The same sort of calculation for M=3 and F=3, gives for the ratio of triple hits and 3 α-particles in different detectors 0.8 (=18−2/((6−1)(6−2))). Comparing the 2 or 3 α-particles coming in different detectors with the 2 or 3 α-particles coming from ^{8}Be or ^{12}C respectively, it is necessary to take care of the Jacobian (a matrix which transforms the 'phase space' of the centre of mass system into the 'phase space' of the laboratory system), which enters into the efficiency of the detectors for the laboratory system. Since the Jacobian is different for ^{8}Be (^{12}C) and for 2 (3) 'independently emitted' α-particles it is hard to evaluate what the ratio should be at lower energies.

For the comparison of the observed energy spectra, taking into account the formulae for the transition probabilities written above, in the case of emission of

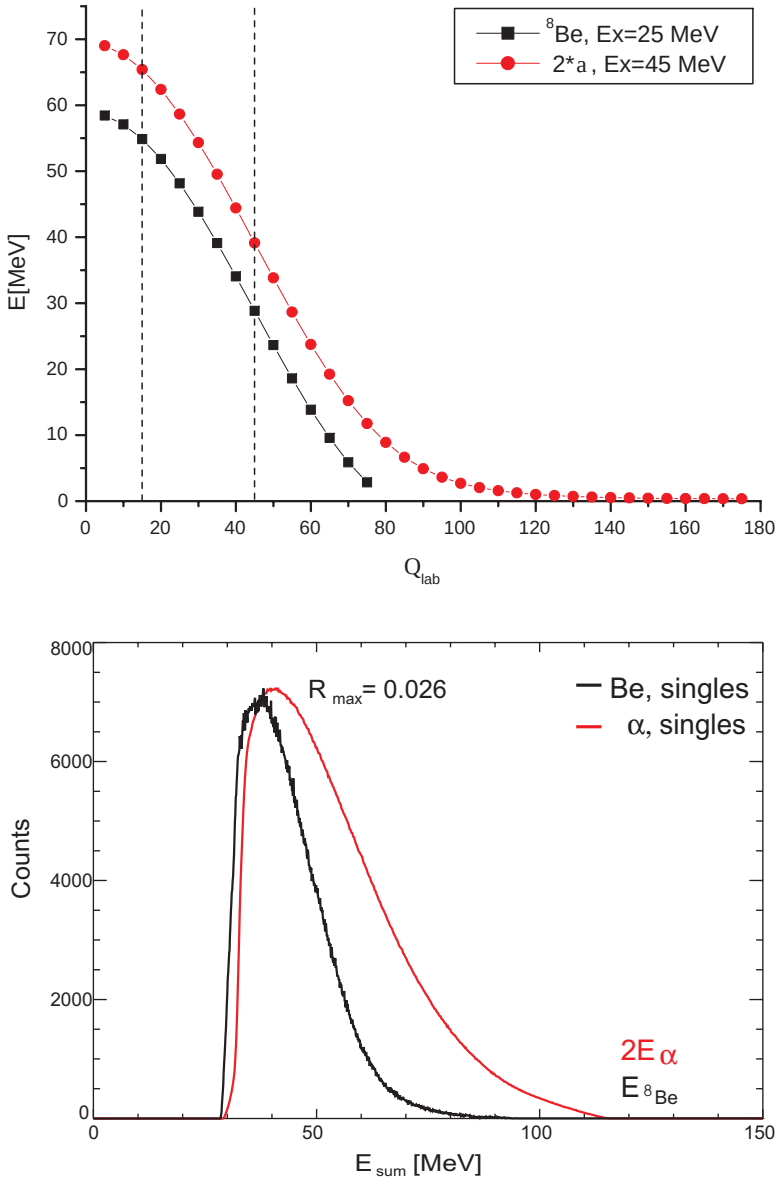

Figure 5.5: Upper panel: kinematical plots for the angular variation of the energy of 2 α's and of ^{8}Be. Lower panel: normalised total energy spectra ($E_{sum} = \Delta E + E$) as observed with the ISIS-charged particle detector system for the emission of single α's, and of ^{8}Be, in the reaction ^{18}O+^{13}C.

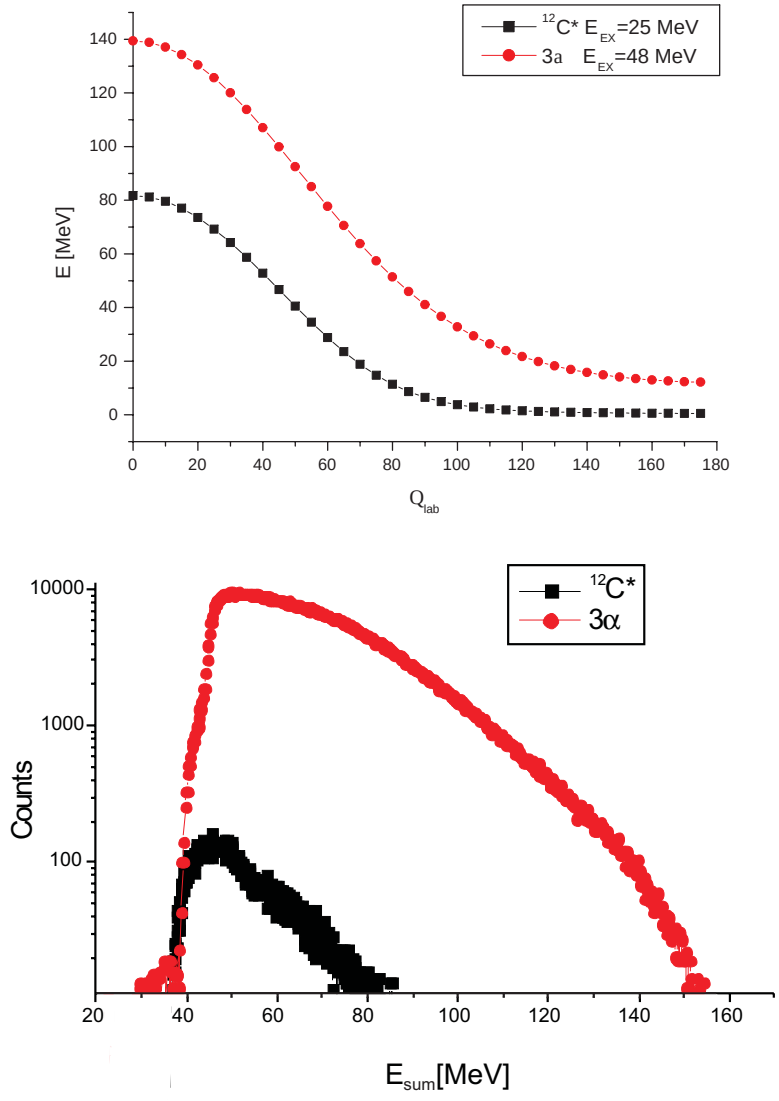

Figure 5.6: Upper panel: kinematical plots for the angular variation of the energy of 3 α's and of ^{12}C$^{*}(0_2^+)$. Lower panel: total energy spectra (ΔE+E-signals) as observed with the ISIS-charged particle detector system for the emission of 3 single α's, and of ^{12}C$^{*}(0_2^+)$ in the reaction ^{28}Si+^{24}Mg.

Jacobian			
J^a_α	1.9	$J_{^8Be}$	2.7
J^b_α	2.1	$J_{^{12}C}$	3.0

Table 5.1: The different Jacobians for both reactions, 'a' for ^{18}O + ^{13}C and 'b' for ^{28}Si+^{24}Mg.

2 α-particles one can obtain:

$$\frac{N^*_{^8Be}}{N^*_{2\alpha}} = \frac{N_{^8Be}}{N_{2\alpha}} \frac{1}{(N-1)} \frac{J_{^8Be}}{\varepsilon (J^a_\alpha)^2} \tag{5.15}$$

where $N^*_{^8Be}$ and $N^*_{2\alpha}$ are the experimentally observed counting rates for ^{8}Be and 2α respectively and $J_{^8Be}$ and J^a_α are the corresponding Jacobians. In Fig. 5.10 (lower panel) shows the experimentally deduced ratio between ^{8}Be and 2 α-particles. It can be seen that the experimentally observed probability ratio between two statistical (uncorrelated) α-particles in one detector and two α-particles in two different detectors (F=2) is an order of magnitude smaller than the expected ratio (0.02 instead of 0.2). The explanation of this experimental fact is that in the emission of 2 α-particles from a compound nucleus it is very unlikely that the second particle will be emitted in the same direction as the first one due to correlation effects; thus the main intensity observed is due to ^{8}Be.

Another important aspect in the discussion of the energy spectra will be connected to the kinematics of the reactions with the emission of the total masses A=4, A=8 or A=12 fragments. The corresponding curves are shown in Fig. 5.5(upper panel) for the relevant angles of the first 3 ISIS rings of telescopes, containing ≈97% of the total multiple hit events. A similar calculation is shown for the second reaction in Fig. 5.6(upper panel). To obtain the Q-value it is necessary to assume a certain excitation energy of the residual nucleus. This implies a prior knowledge of the energy (on average), which is carried away. This can be taken from the systematics of compound decays studied in the same mass

region by Morgenstern *et al.* [Mor83]. In this work the average energy removed by an α-particle is deduced to be 22.1±1.5 MeV and for an individual nucleon 16.4±0.3 MeV. These values are in good agreement with most statistical model calculations.

After considering the different kinematical dependences of the binary emission process we can compare the spectra of ^{8}Be (^{12}C) with the rescaled single α-energy spectrum of the 2 (3)α-particles. This is shown in Fig. 5.5 for the (^{18}O+^{13}C) reaction and for the second reaction (^{28}Si+^{24}Mg), which shows the unbound ^{12}C fragment, in Fig. 5.6.

5.2.2 Gamma-ray coincidence spectra for different fragments

The γ-ray analysis for both reactions will enable the emission mechanism for the different channels to be discussed. In the off-line analysis the different reaction channels were selected by requiring that only the events corresponding to the detection of the proper number of α-particles and protons in the ΔE-E silicon telescopes were incremented into a symmetrised $E_\gamma - E_\gamma$ matrix.

Gamma-ray coincidence spectra following the emission of ^{8}Be and ^{12}C

We are interested in the angular momentum and the energy balance of the binary processes. The first step is to look into the relevant γ-spectra which belong to a given residual nucleus and a given charged particle trigger. Generally, there are still many reaction channels within a charged-particle ISIS-trigger and additional γ-ray gates are needed to identify one residual nucleus uniquely. For the first reaction we have just 2 possible triggers - 2 α particles and ^{8}Be emission, but for the reaction ^{28}Si+^{24}Mg $\rightarrow$^{40}Ca the γ-ray spectra can be obtained with 3 different charged particle triggers a) 3 α particles, b) ^{8}Be+α particle emission, and c) ^{12}C$^{*}(0_{2^{+}})$ emission.

The relatively high velocity of the compound nucleus and the larger mass of the emitted fragments, means that the γ-ray spectra must be Doppler corrected. This correction was carried out by using the sum of the vectors of the coincidently registered charged particles (for more details see Section 2.3.3.). A satisfactory Doppler shift correction was obtained, resulting in an energy resolution of about 10 keV FWHM at 1000 keV.

First the ^{28}Si+^{24}Mg reaction will be discussed, where ^{8}Be and $^{12}C^{*}_{0+}$emission was observed. The detailed spectroscopy of the dominant residual nuclei ^{40}Ca and ^{42}Ca is given in Ref. [Tor03]. Of particular interest here are the differences, which could be observed in the three various charged particle triggers leading to $^{40-42}$Ca as well as to ^{39}K. The results for the ungated γ-ray spectra with the different charged particle triggers are shown in Fig. 5.7.

In both reactions, as previously observed for ^{8}Be emission [Thu99], the binary cluster channel carries less energy and less angular momentum from the residual nucleus than the sequential α-particle emission. Therefore, subsequent neutron and/or proton evaporation becomes more conspicuous. This is particularly visible for the ^{12}C emission (see Fig. 5.7), where the residual nucleus has enough energy even for the subsequent emission of 2p+2n or an α-particle, which leads to ^{36}Ar.

The same result is observed in the ^{18}O+^{13}C reaction (see Fig. 5.8), where the γ-ray spectrum gated on ^{8}Be shows a stronger population for ^{21}Ne, which corresponds to a subsequent neutron evaporation, when compared to ^{22}Ne. Furthermore, using γ-particle coincidences it was possible to investigate the energy dependence of the relative population of these nuclei by gating on different energies for the 2 α-particles, registered in the same detector. As can be seen from Fig. 5.9, the ^{8}Be events are concentrated in the low energy region of the E_{sum}. This is in good agreement with the curve shown in Fig. 5.10, corresponding to the ratio between the rates of the 2 α-particles registered in different detectors and in the same detector, as function of the energy.

Having only statistical (uncorrelated) 2 or 3 α-particles as multiple hit events

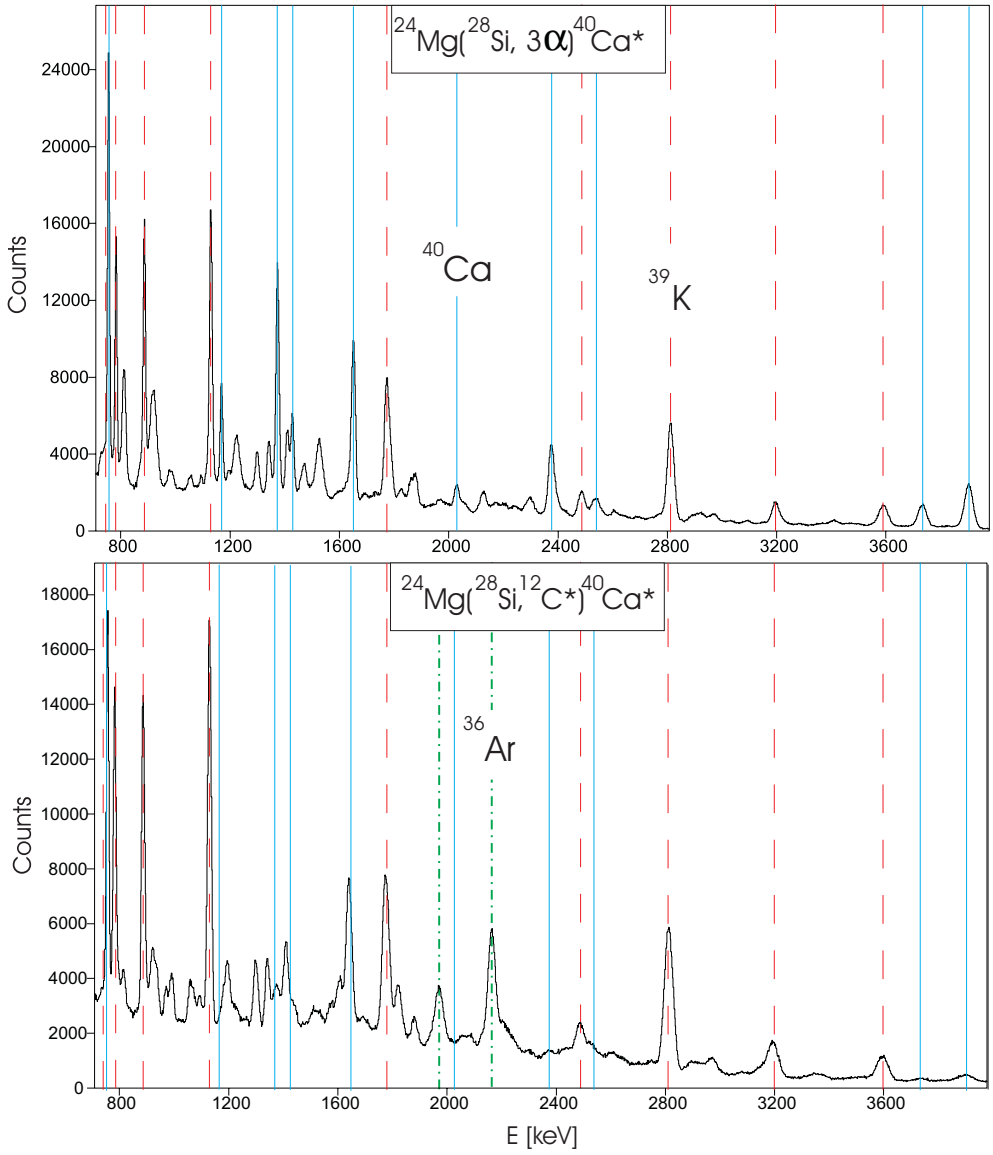

Figure 5.7: Gamma-ray spectra obtained from the ^{28}Si+^{24}Mg reaction gated by different charged particle triggers. Upper panel: Doppler corrected γ-ray spectrum gated by the 3 α channel. Lower panel: Doppler corrected γ-ray spectrum gated by the ^{12}C$^{*}(0_2^+)$ channel.

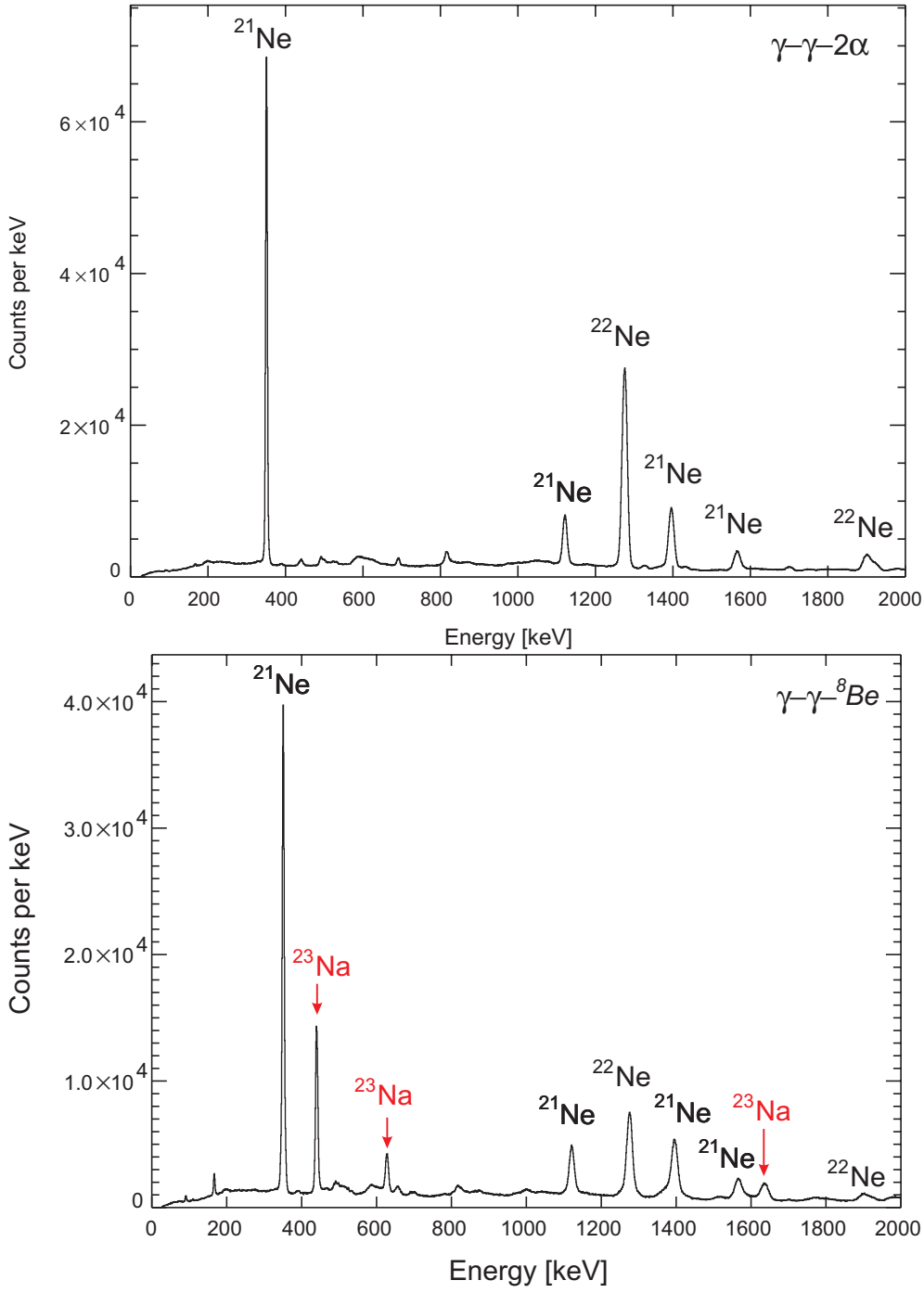

Figure 5.8: Gamma spectra from the ^{18}O+^{13}C reaction gated by different charged particle triggers. Upper panel: Doppler corrected γ-spectrum gated by the 2 α channel. Lower panel: Doppler corrected γ-ray spectrum gated by the ^{8}Be channel.

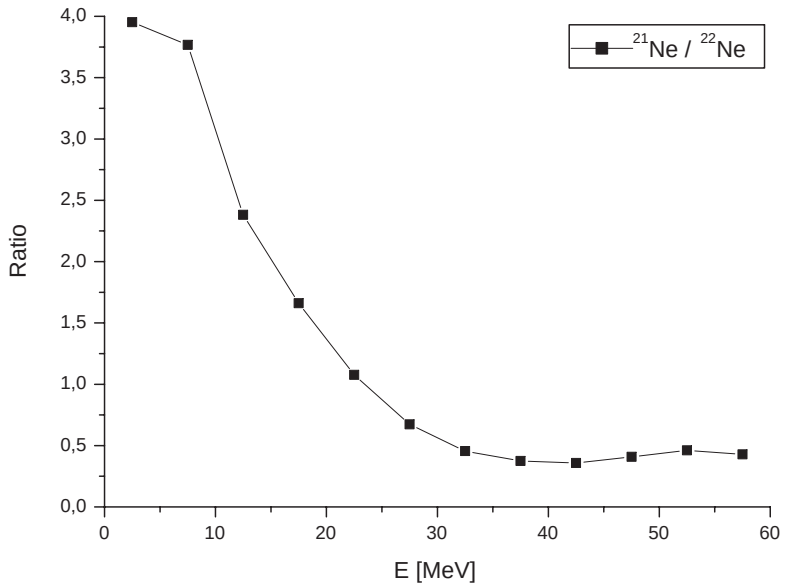

Figure 5.9: Ratio between the populations of the ground state transition in ^{21}Ne (350 keV) and ^{22}Ne (1274 keV) for different energies of the coincident 2 α-particles.

no variation should appear in the ratios given in Figs. 5.10 and 5.11. From both pictures one can see that the clusters are concentrated in the low energy region where the biggest deviation from a horizontal line is observed. In both cases the ratios go well below the expected multiple hit level (factor 10 to 100) indicating that the multiple hit events can be neglected in the ^{8}Be and ^{12}C spectra. This is confirmed by the study of the γ-decays.

With the observation of various channels like 2α, 3α, ^{8}Be or ^{12}C a systematic dependence on the excitation energy in the residual nucleus in cluster emission can be found. Note once more that in the systematics of Morgenstern *et al.* [Mor83], the average energy carried by individual nucleons and α-particles is compared. Each individual nucleon carries approximately 16.4 MeV (four nucleons 66 MeV), one α-particle carries approximately 22.3 MeV. Subtracting the α-particle binding

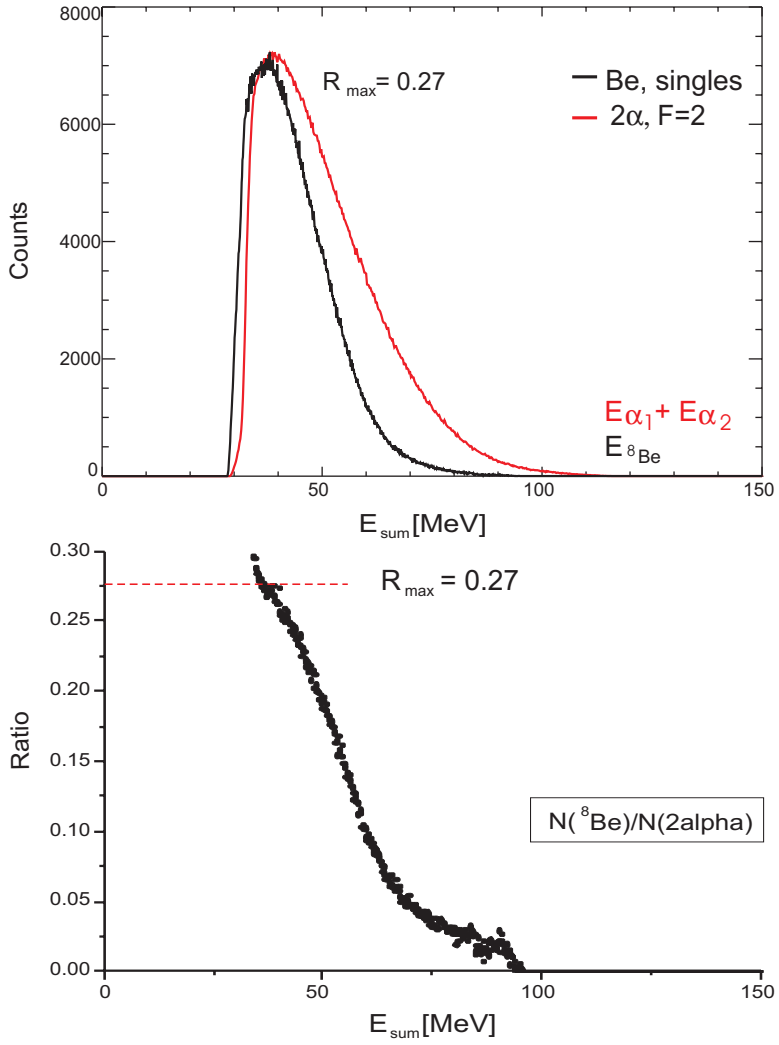

Figure 5.10: Upper panel: the normalised total energy spectra ($E_{sum} = \Delta E + E$) as observed with the ISIS-charged particle detector system for the emission of 2 single α's, and of ^{8}Be, in the reaction ^{18}O+^{13}C. Lower panel: the ratio between these two experimental curves.

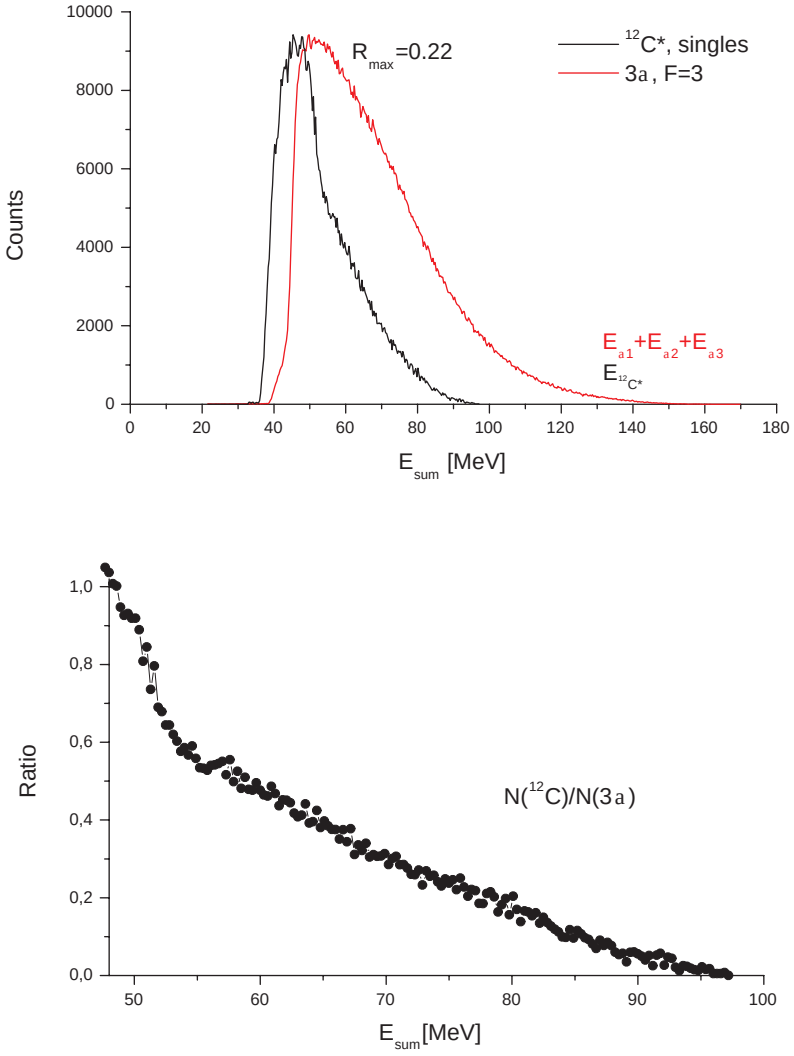

Figure 5.11: Upper panel: the total energy spectra ($E_{sum} = \Delta E + E$) as observed with the ISIS-charged particle detector system for the emission of 3 single α's, and of ^{12}C, in the reaction ^{28}Si+^{24}Mg. Lower panel: the ratio between these two normalised curves.

energy of 24 MeV, the 4-nucleons should have carried away 42 MeV, much more than the 22.3 MeV of the four bound nucleons. In addition, the unequal energies carried by single protons, and neutrons of 18.3 MeV and 13.2 MeV [Mor83], respectively, point to the influence of the Coulomb barrier, E_{CB}. The Coulomb barrier shifts the maximum energy expected for the emitted particle to larger values. Because of the linear dependence of the value of E_{CB} on the emitted charge one can expect that the cluster emission energy spectra will be only slightly shifted to higher energies. The E_{CB} for ^{8}Be and 2 α-particles for example has a difference of $\approx$2 MeV (higher for ^{8}Be). What one can see from the data is the opposite effect (see Figs. 5.5(lower panel) and 5.6(lower panel)): in both cases the maxima of the cluster emission energy spectrum is shifted to lower energies. One possible reason for this could be the difference coming from the kinematical variation of the energies (see Figs. 5.5(upper panel) and 5.6(upper panel)). Another possible explanation is given below.

The relative population of transitions following different decay modes, or alternatively, the ratio of the sequential emission to the binary cluster emission for a particular region in the decay scheme will be discussed. For the discussion the standard formulation for the energy spectra of evaporated particles can be used. The energy carried away in one evaporation process is given by Equation 5.16.

$$P(E) = E((2J+1)/12)\sqrt{a}\exp\sqrt{4a(E-E_{rot})}. \tag{5.16}$$

Here, J is the spin, E_{rot} is the rotational energy and a is the level density parameter. One of the clearest features of the sequential emission is the fact that the level density enters into each decay process, implying that in the sequential emission the decay phase space enters several times. Therefore, the sequential decay will dominate over the cluster decay. However, special effects like strong deformation or clustering in the parent nucleus may enhance the emission of larger fragments. Results concerning the population of deformed bands in ^{48}Cr by the emission of ^{8}Be from the compound nucleus have been studied with a similar procedure

using the GASP-ISIS-detector set-up and have been described by Thummerer *et al.* [Thu01].

Another important feature of the chosen reaction channels is the selective population of states with natural parity in the residual nucleus, if only particles with spin zero, like the ^{8}Be and ^{12}C fragments, are emitted (see discussion on ^{40}Ca parity doublets by Torilov *et al.* [Tor03]).

A pronounced difference in the excitation energy of the residual nucleus for the emission of clusters compared to the sequential processes has been observed. The relative yields are given (see Fig. 5.12) for the decay chains (3α, ^{8}Be+α or ^{12}C), for the ^{28}Si+^{24}Mg reaction. By inspecting the gated spectra one can see that the relative and absolute intensities of the lowest lying γ-ray transitions in ^{40}Ca and ^{39}K (the latter being indicative of a subsequent decay) are populated differently in the various particle gates. This is due to differences in the excitation energy and angular momentum in the residual nucleus ^{40}Ca.

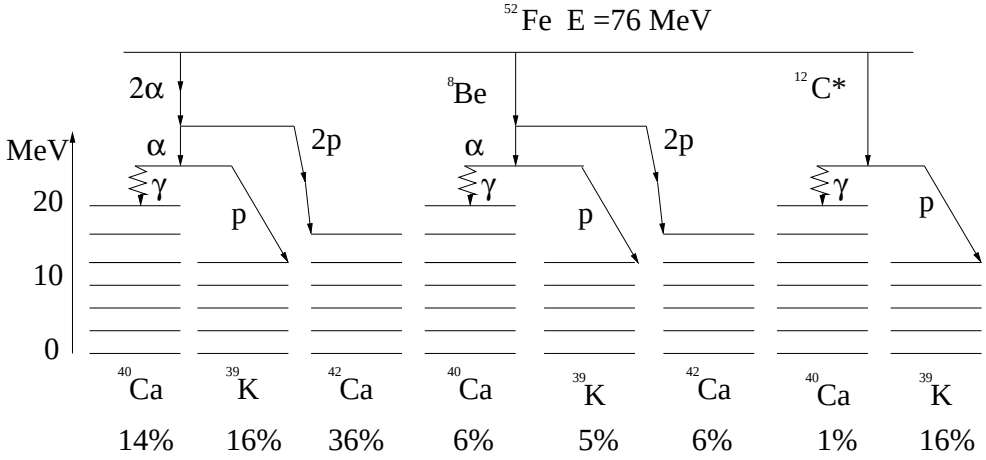

Figure 5.12: Intensity fractions for γ-ray transitions in residual nuclei gated by the 3α, (^{8}Be+α) and ^{12}C$^{*}(0_2^+)$ channels from the ^{28}Si+^{24}Mg reaction.

Similarly, for the ^{13}C+^{18}O reaction, the relative strengths of the subsequent neutron decays have been compared following the emission of 2 α's, or a ^{8}Be, namely, the 0n, 1n and 2n channels, populating the residual nuclei ^{23}Ne, ^{22}Ne, and ^{21}Ne respectively. As can be seen from Fig. 5.8 in the coincidence γ-ray spectra

with '^{8}Be' the subsequent neutron emission is enhanced. Comparing the γ-ray spectra triggered on 2 α-particles (Fold=2) the ratio between the population of ^{22}Ne (ground-state transition) in both matrices is $\approx$4 and for ^{21}Ne (ground-state transition) only $\approx$1.5. (The total ratio of events N(2α)/N('^{8}Be')$\approx$1.5).

Gamma-ray coincidence spectra following the emission of ^{6}Li and ^{7}Li

In the second reaction (^{18}O+^{13}C) it can be seen (Fig. 5.13) that the calculated points of the energy loss of different fragments when flying through the silicon-telescopes are in good agreement with the experimental spectra. In Fig. 5.8 the γ-ray spectra gated by two α-particles in different detectors and by two α-particles coming in the same detector are shown. Looking at the spectra an interesting phenomenon was observed. Checking the γ-ray transitions which are observed in coincidence with the peak at 439 keV proves that the peak is the transition from the first excited state to the ground state in ^{23}Na. From the charge conservation law it is not possible to have sodium (Na, Z=11) after the evaporation of 2 α-particles from Si (Z=14). This experimental observation was carefully investigated and analysed. In the 2 α-gated spectra (F=2) this peak (439 keV) is very weak (see Fig. 5.8), which is expected, after the suppression by the particle gate condition. In contrast, in the '^{8}Be' gate this peak is very strong and other peaks from the same nucleus (^{23}Na) are observable (see Fig. 5.8). This effect is presumably due to lithium emission, overlapping with the ^{8}Be particle gate. This hypothesis is tested below. In addition, the population of ^{21}Ne relative to ^{22}Ne increases when gating on ^{8}Be rather than 2α-particles (Fig. 5.9).

In order to investigate this the '^{8}Be' banana was cut in energy steps of 5 MeV and the γ-ray coincidences were analysed (see Fig. 5.14). One can see that ^{8}Be is stronger by a factor of 2$\rightarrow$2.5 than the lithium. Further examining the ratios between the different neon-isotopes and sodium (see Fig. 5.15) one can see that the lithium is stronger at lower energies. Thus, looking at the energy spectra for 2 α-particles registered in the same detector, a possible 'scenario' for the

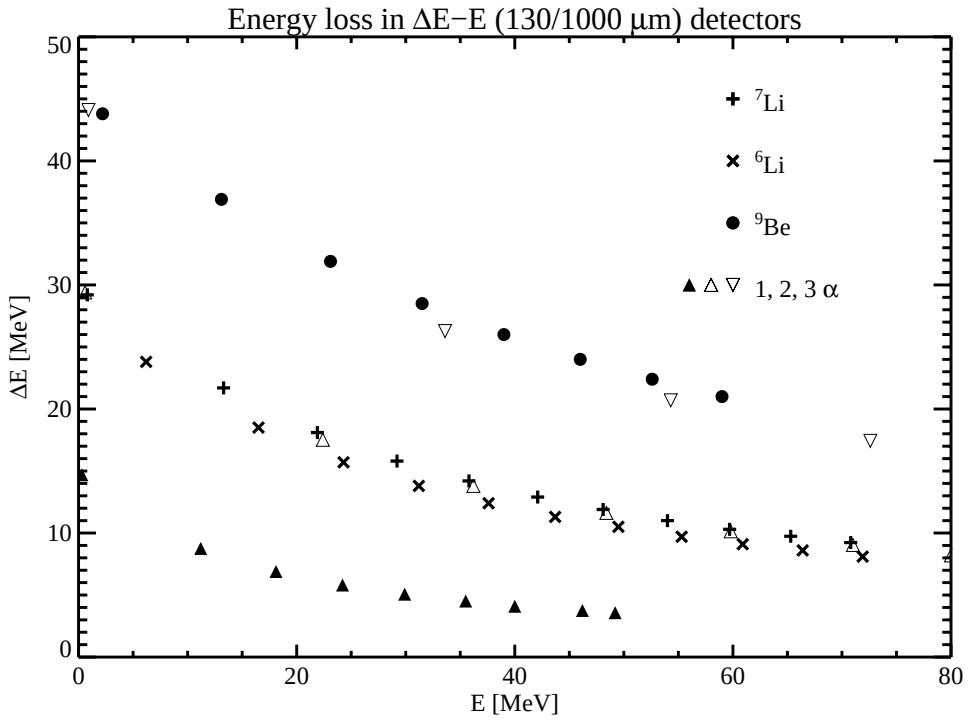

Figure 5.13: Calculations for the energy loss of different charged particles and clusters in the silicon-detector telescopes.

cluster emission can be constructed: At lower energies presumably the emission of ^{6,7}Li and ^{8}Be is dominant, rather than mainly ^{8}Be and some 2 uncorrelated (chance) α-particles; in the highest energy region mainly 2 uncorrelated (double hit) α-particle events are dominant.

5.2.3 Energy-to-angular momentum balance

By looking at the energy-to-angular momentum balance for the sequential emission processes versus the binary reactions the differences observed in the population of the final states in the residual nuclei (^{23}Ne and ^{40}Ca) and the probability of a subsequent decay (because of a higher residual excitation energy) can be discussed further. The first step is to consider the angular momenta carried by, for example, 2 α-particles or a ^{8}Be cluster. The formula for the angular momentum,

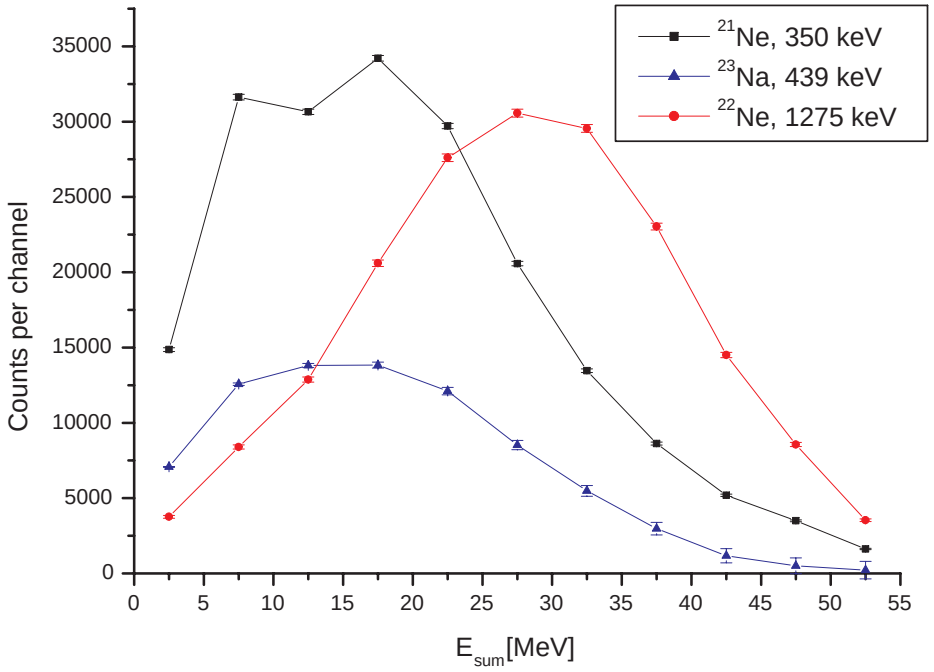

Figure 5.14: Distribution of the populations of the ground-state transitions in ^{21}Ne (350 keV), ^{22}Ne (1274 keV) and ^{23}Na (439 keV) for different energies of the coincidence gate ('^{8}Be'+ double hit events).

L_x, of a fragment, x, for a given kinetic energy, E_x, is given by Equation 5.17.

$$L_x = kR\sqrt{1 - \frac{E_b}{E_{CM}}} \tag{5.17}$$

where E_b is the binding energy and the wave number k is given by the product of mass times kinetic energy (as used in Equation 5.18). The α-particle has mass, m_1, and an average energy, E_1. If the larger cluster consists of 2 α-particles, the total mass is $2m_1$, and if the kinetic energy of the cluster is twice the energy of a single α-particle emitted in the sequential process, there is no difference in the energy-to-angular momentum balance of the reaction according to Equation 5.17.

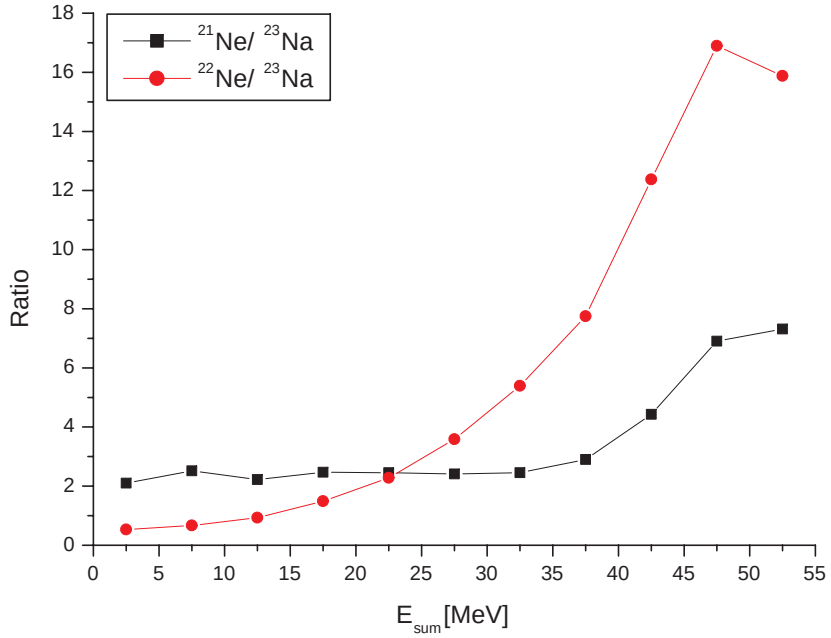

Figure 5.15: Ratio between the populations of the ground state transitions in ^{21}Ne (350 keV), ^{22}Ne (1274 keV) and ^{23}Na (439 keV) for different energies of the coincidence 2 α-particles registered in the same detector. The curve is expected to give a horizontal line for pure double hit events (corresponding to the ratio between the probability of 1 and 2 neutron emission).

$$k_{^8Be} = \frac{\sqrt{4m_1 2E_1}}{\hbar} = 2k_\alpha \tag{5.18}$$

The origin of the difference in the population of the residual nucleus in a sequential compared to a one-step evaporation process for the same mass must be found in the emission process itself. There are two potential origins of the difference,

a) less angular momentum is carried away in the one-step process, because the geometry is more like a sticking situation, as in fission, or

b) in the sequential process, because of the dependence on the level density

(which enters two or three times for 2 or 3 α-particles respectively) the emission of more total energy is emphasised.

5.3 Conclusions

The cluster fragments, ^{8}Be or ^{12}C carry away less energy from the compound nucleus than 2 or 3 sequentially emitted α-particles and in the cluster scenario, corresponding to the same total (A,Z), the emission of another light charged particle from the residual nucleus is enhanced. The higher probability of sequential α-particle emission than of cluster emission, is in good agreement with the statistical model. In terms of angular momentum, 2 α-particles will have a higher total angular momentum because they carry more energy. Furthermore, in the sequential process the level densities emphasise the emission of higher total energy of the α-particles.